DICOM File for Total Body Photography: a work item proposal

Wei-Lun Huang[a,d], Shuya Liu[b], Jun Kang[c], Amir Gandjbakhche[d], and Mehran Armand[a,b,e]

[a]Johns Hopkins University, Whiting School of Engineering, Department of Computer Science, Baltimore, MD, USA
[b]Johns Hopkins University, Whiting School of Engineering, Laboratory for Computational Sensing & Robotics, Baltimore, MD, USA
[c]Johns Hopkins School of Medicine, Department of Dermatology, Baltimore, MD, USA
[d]Eunice Kennedy Shriver National Institute of Child Health and Human Development, Bethesda, MD, USA
[e]Johns Hopkins School of Medicine, Department of Orthopaedic Surgery, Baltimore, MD, USA

ABSTRACT

Total-body photography (TBP) has gained increasing attention for facilitating early melanoma detection. TBP has advantages of monitoring temporal changes in lesions, screening a large number of lesions efficiently, and providing anatomical locations for dermatoscopic images. Since various digital imaging systems for TBP have been proposed, there is a need for a unified format for the storage of the data from TBP. Digital Imaging and Communications in Medicine (DICOM) is the international standard for medical imaging. Thanks to a considerable effort to develop dermatology-specific extensions to the DICOM standard, there is a recent supplement to the DICOM standard for individual dermoscopic images. This supplement, however, does not cover the requirements for TBP, which may include multiple wide field-of-view images. Moreover, TBP may be obtained using various methods i.e. the images can be acquired with either consumer-grade cameras, smartphones, or an automatic scanning machine. This paper provides an overview of the specific requirements and an outline of a "Work Item" leading to a Total Body Photography Information Object Definition (IOD). The "Work Item" is inclusively designed for accommodating current variants of TBP data to be compatible with the DICOM standard for dermoscopy and applicable to future systems and other potential use of TBP. We verified the feasibility of the proposed TBP DICOM in an imaging-rich full-body scanning system.

Keywords: DICOM, Total Body Photography, Skin Cancer

1. INTRODUCTION

Skin cancer is the most commonly diagnosed cancer in the United States. Among all skin cancer cases, invasive melanoma accounts for the vast majority of skin cancer deaths. In 2021, melanoma-related cancer is estimated to have increased by 100000 cases and caused more than 7000 deaths [1,2]. Early detection of melanoma is critical for improving patient outcome [3].

Total-Body Photography (TBP), a method that photographically documents a person's entire cutaneous surface through a series of body sector images, is becoming commercially available as an aid for early melanoma screening in high-risk persons [4]. A recent study has shown that TBP can help detect potential melanomas by monitoring high-risk patients with follow-up visits to improve overall survival rate [5]. TBP allows the longitudinal tracking of the change of pigmented skin lesions (PSLs), namely "evolution", as an additional risk factor for melanoma [6]. TBP provides an efficient way to screen a large number of lesions with its wide-view pictures. It can also be used for detecting lesion saliency (also known as ugly duckling criteria) for assessing

Send correspondence to Wei-Lun Huang, E-mail: wl.huang@jhu.edu

suspicious skin lesions.* In current practice, TBP is usually combined with Sequential Digital Dermoscopy Imaging (SDDI) to provide anatomical locations for sequential digital follow-ups [8].

Many specialized systems have been developed for image acquisition, storage, and retrieval that allow physicians to manage TBP assisted follow-up and sequential digital dermoscopic monitoring. A number of commercialized TBP systems are available in the US market such as Canfield Vectra 360, FotoFinder Bodystudio ATBM, MelanoScan, and Microderm, which include both automated and manual capturing procedures. For automated devices, they usually come with a PC workstation for controlling the scanning pipeline. For manual capture, the manufacturers may provide a convenient handheld device or allow physicians to photograph lesions with their own cameras. On the other hand, in the research field, there are image-based and 3D-mesh-based TBP systems. Dengel et al. [9] prototyped a rapid TBP imaging system with adequate lesion visualization and high participant acceptance. They used 16 cameras to acquire multiple photos of patient skin in two poses for complete coverage. Korotkov et al. [10] designed a TBP system with 21 high-resolution cameras and a turntable, which could map PSLs automatically and estimate lesion change using a set of overlapping images. Bogo et al. [11] developed a multi-camera 3D stereo system for detecting new lesions or growth in existing ones. They captured 3D textured scans of a subject and represented the scan in a parametric 3D body model to make the lesion tracking robust to changes in illumination and subject pose. Recently, Zhao et al. [12] used a handheld structured light 3D scanner to acquire a 3D textured mesh for tracking longitudinal skin lesions. Lesions of the total-body skin were first detected on 2D texture images, then were mapped back to the 3D mesh surface of the subject.

Since different digital imaging systems for TBP generates its own output data, 2D images and/or 3D surface mesh, there is an unmet need for a unified format for storing data from TBP. Especially with the growing popularity of machine learning (ML) and artificial intelligence (AI) applications in dermatology, the method for storing standardized image along with formatted metadata has an unmet need to enable the AI applications [13, 14]. Digital Imaging and Communications in Medicine (DICOM) is the international standard for medical imaging [15]. It is one of the most widely used standards in healthcare defining formats for images and structured data. Thanks to a considerable effort to develop dermatology-specific extensions to the DICOM standard, there is a recent supplement to the DICOM standard for individual dermoscopic images [16,17]. However, the mentioned "Work Item" does not cover the requirements for TBP. Multiple wide field-of-view images should be included in TBP DICOM. Since [17] is specifically designed for images acquired by dermoscope, a more comprehensive structure is crucial for TBP systems that use digital camera or smartphones to capture images.

In this paper, we provide an overview of the specific requirements and functions of Total Body Photography and an outline of a "Work Item" leading to a Total Body Photography Information Object Definition (IOD). We propose a structure for storing data that supports both 2D images and 3D surface mesh of the patient, as shown in Fig. 1. We also provide a workflow to guide the inclusion of TBP data into DICOM format as will be discussed in section 2.3. The "Work Item" is designed to not only accommodate current variants of TBP data but also be compatible with the DICOM standard for dermoscopy. In Fig. 1, each DICOM file with a dermoscopic image can be associated to a TBP DICOM file following the standard. Finally, the proposed structure would be applicable to future systems and other potential use of TBP. We verified the feasibility of the proposed TBP DICOM with an imaging-rich full-body scanning system and provided examples of use cases.

2. METHOD

2.1 DICOM and DICOM Metadata

DICOM is a comprehensive, international medical image management standard that defines standardized, structured, and coded metadata models that are patient-, modality-, and specialty-specific. The DICOM metadata includes the patient, study, series, and other technical metadata that are necessary for clinical imaging. The definition of an instance of DICOM metadata is called **Information Object Definition (IOD)**. IOD is an object-oriented abstract data model used to specify the information about real-world objects such as X-rays and MRI. The **attributes** of an IOD describe the properties of a real-world object instance. Related attributes are grouped into **modules** that represent a higher level of semantics documented in the module specifications. A

*Highly accurate and skilled clinical detection of melanoma appears to rely heavily on unconscious visual pattern and comparative "ugly duckling" recognition [7].

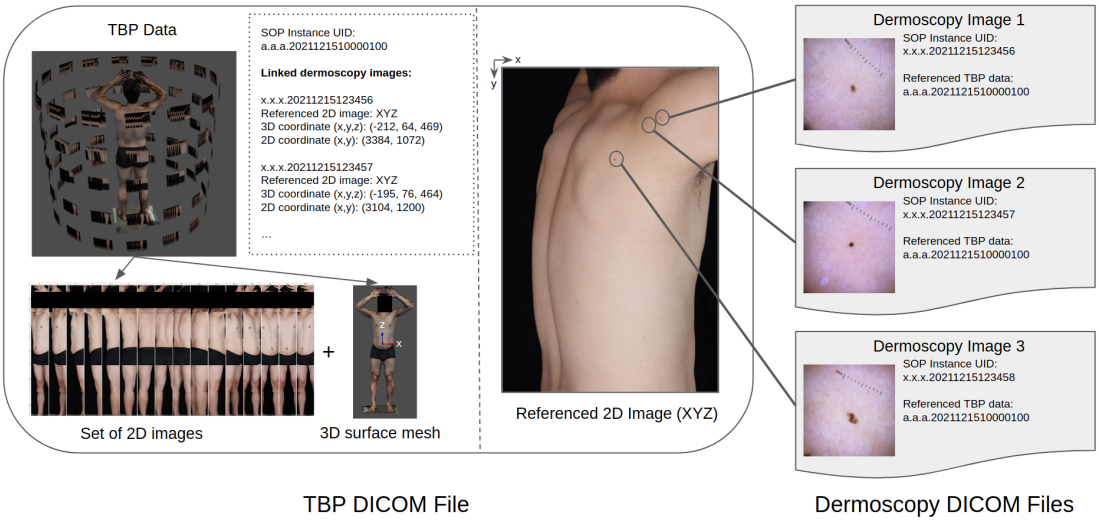

Figure 1. A TBP DICOM file and its relation to Dermoscopy DICOM files

group of modules are labeled as **Information Entity** that is related to one specific class of real-world object, such as patient, study, and series. The object-oriented design of the metadata model enables modules to be reused in different IODs, resulting in efficient creation for new IODs. A **Service-Object Pair (SOP)** Class is defined by the combination of an IOD and service elements such as storage, move, print, or query. A DICOM file is an SOP instance with **SOP instance unique identifier (UID)**. The following sections of this paper frequently refer to these terminologies as defined in DICOM. Referenced IODs, modules, and attributes as defined in DICOM are highlighted in bold-case.

2.2 Functions of TBP

Before outlining the structure of a TBP IOD, we will first discuss several functionalities and potential use cases that TBP data can provide. The TBP IOD needs to be designed to not only suffice the requirements but also be easily adapted for the future advancement in TBP systems.

2.2.1 Anatomical record

The lesion of interest should be recorded anatomically in the TBP data for unique identification and future revisit. To more precisely describe the location of the lesion, the 2D- and 3D-coordinate of the lesion should be provided in 2D images and 3D surface mesh, respectively. The 2D image can be referred as a regional image that includes anatomic reference points, such as joint or navel, within the field of view. The generation of the coordinates of the lesion can be as easy as using input devices (e.g. mouse, keyboard, touch screen) pointing on the image or mesh of the TBP data [17]. If the camera parameters can be estimated and the spatial relationship of 2D images and 3D mesh are known, the 2D-coordinate and 3D-coordinate of the lesion can be mapped through a pinhole camera model. Given the camera matrix $\mathbf{K}$, a 3×4 matrix as a composite of the camera pose and its intrinsic parameters, for a 3D point $\mathbf{P}$ selected by user, the 2D point $\mathbf{X}$ on the image can be derived as:

$$\mathbf{X} = \mathbf{KP}$$

where $\mathbf{P}$ and $\mathbf{X}$ are expressed in homogeneous coordinates. Since the TBP can be combined with SDDI in clinical settings, the dermoscopic images should be anatomically associated with the TBP data per acquisition. The function of anatomical record should enable a bi-directional data retrieval: from dermoscopic image to TBP data and vice versa.

2.2.2 Wide-view screening

TBP allows wide-view screening if the texture of lesions can be captured with adequate quality. Wide-view screening provides additional helpful context that is not available when only considering a localized lesion at a single point of time, such as ugly duckling criteria*. The screening of the skin lesions can be done either manually by dermatologists or automatically by software systems [10, 18, 19]. A typical automatic workflow would first isolate the skin from background and clothing by thresholding the entire image in the HSV (hue-saturation-value) color space. Then a blob detection algorithm (e.g. based on Laplacian of Gaussians (LoG) and scale-invariant feature transformation (SIFT)) would be applied to extract all regions of interest in an image. The detected regions are subsequently classified to be suspicious lesions or not using a machine learning model.

2.2.3 Longitudinal tracking

TBP preserves the visual information of the entire body surface of a patient. A sequence of TBP scans over time is essential for longitudinal tracking of skin lesions: detecting new lesions and temporal change of prior lesions in size, border, color, and texture. The longitudinal tracking of the lesions involves two steps: matching lesion correspondences across scans and detecting the change. Let $l_t \in L_t$ and $l_{t+1} \in L_{t+1}$ be lesions from two TBP dataset D_t and D_{t+1} for scans at time t and $t+1$, the matching function can be formalized:

$$M : (l_t, l_{t+1}) \mapsto \{0, 1\}$$

which is 1 when l_t and l_{t+1} correspond to the same lesion, and 0 otherwise. A clinician can manually achieve the task by selecting lesion of interest in an individual scan and then examine the lesion from different time-stamps side-by-side. On the other hand, a number of different automated algorithms of lesion tracking has been proposed as well. For 2D images, the lesion correspondence can be matched through a structured graphical model by detecting anatomical landmarks in image and associating lesions with detected landmarks [20]. If the 3D spatial relationship among images and/or a 3D representation of patient data are provided, additional information such as 3D location of the lesion and geodesic distance between pairs of lesions can be used for the matching problem [10–12, 21]. The 3D information can be especially helpful for correspondence matching when the visual appearance of the lesions change over time in different scans. After correspondence is established, lesion segmentation and image registration are required to fix the difference in perspectives before detecting temporal change. An example would be estimating the homography (a 3x3 matrix) as the geometric transformation of the lesion assuming the lesion lies on a plane [22].

2.3 Structure of TBP IOD

The proposed structure of TBP IOD is shown in Fig. 2 (a). Based on DICOM **IOD Entity-Relationship Model** that depicts the relationships of all the components of an IOD, TBP IOD contains essential modules within the **Information Entities** following the hierarchy of patient, study (equipment, frame of reference), series, and other entities. TBP IOD is designed to support both 2D images and 3D mesh by referencing existing IODs. Although either 2D images or 3D mesh is sufficient for total body photography, it is recommended to create data in both modalities to optimize the functionalities of TBP. Often, 2D images preserve sharper texture of skin and lesions over 3D mesh at the same magnification level due to imperfect multi-frame registration and the ambiguity of color information coming from multiple images with different surface reflections. However, a surface mesh provides a 3D coordinate system to precisely describe the location of lesions of interest. The 3D coordinate of a lesion helps to keep track of the lesion temporally. In addition, as opposed to using multiple 2D images with overlaps to construct the body map, 3D model has a clearer structure in its representation and is easier to navigate.

The proposed workflow to encode TBP data is shown in Fig. 2 (b). If a 2D image is acquired by digital cameras of which sensors are sensitive to visible or near-visible light, it can instantiate **Visible Light (VL) Photographic Image IOD**. The IOD has **VL Photographic Acquisition** module to save the image capture conditions such as exposure time, ISO speed, aperture value, focal length, and white balance for the repeatability and comparability of TBP images. In addition, storing the capture conditions at image-level rather than system-level can easily adapt to more complicated design of TBP systems as described in the section 2.3.1. Otherwise, if images are not captured from visible light, we propose to use **Secondary Capture Image IOD** to encode

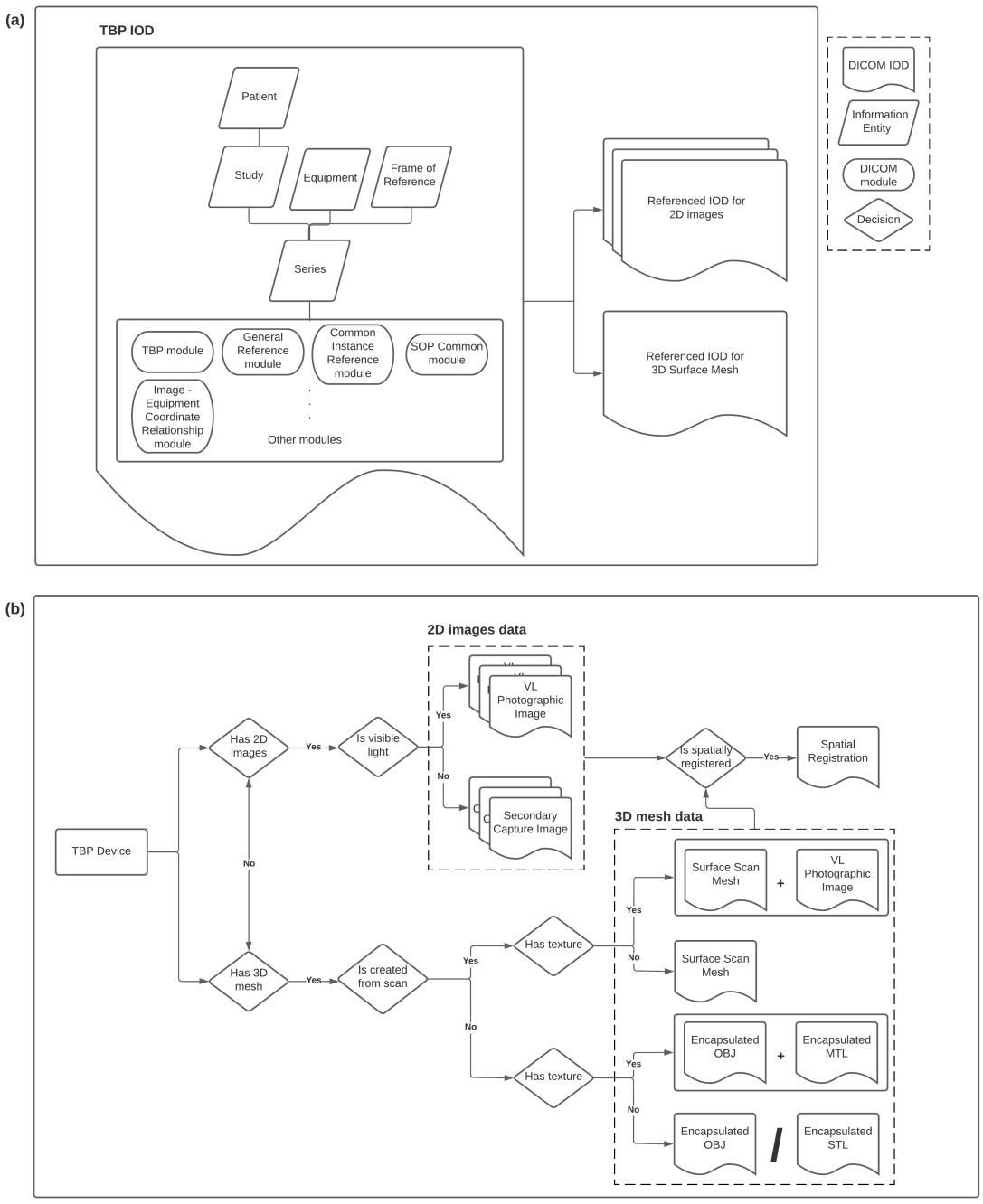

Figure 2. Structure of TBP IOD and workflow to encode TBP data

the data. The IOD is modality-independent and does not have any constraints on pixel data format. As for the 3D mesh of the patient, depending on its creation method, the mesh can instantiate **Surface Scan Mesh IOD**, **Encapsulated OBJ IOD**, or **Encapsulated STL IOD**. **Surface Scan Mesh IOD** specifies a triangulated surface generated by an optical surface scanner or a 3D post-processing application [23]. The surface information, such as vertices position and normal, is stored in the **Surface Mesh** module. The **Scan Procedure** module records the attributes for the surface scanning process. On the other hand, if the 3D mesh is not derived from

a surface scan (e.g. template mesh of human body), we propose to enclose the data in **Encapsulated OBJ IOD** or **Encapsulated STL IOD** since OBJ and STL are two of the most commonly used formats in 3D geometry. For a textured mesh, **UV mapping** module and a linkage to **VL Photographic Image** instance are used along with the **Surface Scan Mesh** instance, while a linkage to **Encapsulated MTL** instance for supporting files such as material library and texture maps is adopted for the **Encapsulated OBJ** instance. It is important to note that in some TBP data, the spatial relationship of 2D images and 3D mesh can be reconstructed. In this case, **Spatial Registration IOD** may be utilized to store the position and orientation of image planes registered to the 3D mesh. DICOM defines the standard Patient-Based Coordinate System, an orthogonal Cartesian right-handed system (unit in mm) with positive x-axis pointing toward left hand side of the patient, positive y-axis pointing toward the posterior side of the patient, and positive z-axis pointing toward the head of the patient, as depicted in Fig. 4 (a). For proper interpretation, **Image - Equipment Coordinate Relationship** module can be used to store a rigid transformation that involves translation and rotation if the equipment coordinate system is different from the patient coordinate system.

TBP module would be a newly proposed module to include important properties of TBP data of which definitions are currently not defined as attributes in DICOM, such as available data format (2D images and/or 3D mesh), TBP capture procedure (enumerate values of instant capture/continuous scanning/other types), body coverage (enumerate values of range of percentage), and linkages to dermoscopy DICOM files (list of annotated lesions). Text descriptions for missing body parts in a TBP scan (e.g. armpit and plantar) should be annotated. If the 3D mesh is in real-world scale, the pose of the patient and the reconstruction error measured from certain body parts should be recorded.

2.3.1 2D Images in TBP

For extensive usages of the 2D images in TBP, the image modules should be capable of including the following scenarios: multi-spectral images, images for focus stacking, bursts of images from slightly different perspectives, and more.

For example, wood's lamp (365nm UV) illumination capabilities are shown to be used for detection of other skin conditions such as solar elastosis that may serve as biomarkers for skin cancer risk [24] and cutaneous pigmentary disorders [25]. Therefore, a TBP system can capture images of the same region under other illuminations other than the white color. The light source and the spectral sensitivity of each channel of the camera used are all included in the **VL Photographic Acquisition** module. As another example, as polarized light effectively eliminate the reflections on the skin surface and is widely adopted in dermoscopy, the **Polarization** attribute is created in [17] and can be used in a TBP DICOM file.

Since the depth of field is limited for camera and becomes smaller as the focus distance gets shorter, blurring in images of body regions that are outside the camera's depth of field can occur during the TBP image capture process [10]. For example, when a camera is capturing from the lateral side of a patient, one thigh that is closer to the camera would be in focus while the other is not. Hence, to extend the depth of field, a system can potentially capture images at different focus distances for a surface with a large variation in depth.

As wide-view screening is a major advantage of using TBP, improvement in image quality, resolution and clarity in detailed texture, is desired as the TBP system evolves. In addition to enhancement in hardware design, such as image sensor and lens, multi-frame/single-frame image super-resolution is another direction to enhance the visual perception of images [26, 27]. Multi-frame super-resolution, a technique that aggregates the pixel information from multiple images after image alignment, outperforms its counterpart single-frame super-resolution that is limited to prior information within a single image. Therefore, a TBP system can be deliberately designed to capture burst of images from slightly different perspectives to facilitate super-resolution.

A representative image can be selected from similar images, using the **Reference Image Sequence** attribute in **VL Image** module to reference other images significantly related to this image. On the other hand, a derived image may use **Source Image Sequence** attribute in **General Reference** module to specify a set of images that were used to derive this image.

2.3.2 3D Surface Mesh in TBP

A 3D surface mesh may not be directly provided from a TBP scanning process. Therefore, we enumerate several methods to create 3D meshes as a reference. Photogrammetry-based reconstruction is a method to generate the geometric 3D shape of an object from a series of pictures taken from different viewpoints [28]. Without any prior information, it starts with "Structure from Motion" [29] to estimate all the camera poses, camera intrinsic parameters, and a sparse reconstructed point cloud. The multi-view stereo step further densifies the point cloud, estimates a best-fitting surface mesh, and finally texturizes the mesh. Generated mesh can be enclosed in **Surface Scan Mesh IOD** or **Encapsulated OBJ IOD**.

Despite of its easiness and decent quality, the photogrammetry-based approach requires a certain amount of overlaps across images, and its speed is dependent on the number of images and image resolutions. Another method uses depth cameras to perform 3D scanning of the subject [30]. This method accumulates the point cloud from multiple depth images from different viewpoints to generate a 3D surface mesh. A textured mesh can also be generated using RGB-D cameras. This approach is fast as the mesh can be generated immediately after capturing the images. However, the quality of the reconstructed mesh depends on the quality of the depth images.

The generation of parametric models is another approach to generate 3D human body based on statistical analysis of 3D body training data [31]. Starting from a template mesh of human body, a typical parametric model deforms the mesh by identity-dependent body shape and pose-dependent articulated deformation built upon a set of joint angles and bone lengths. The model has limited expressiveness but is largely improved by data-driven analysis to capture the correlations of shape deformations between different individual bodies as well as correlations of pose deformations. The method also has the robust ability to complete a 3D body model from incomplete data, while the previous two methods may suffer from having holes and gaps in the mesh due to self-occlusion and inaccessibility of places. The created mesh from parametric models must be stored as an **Encapsulated OBJ** instance or an **Encapsulated STL** instance. Since the mesh from parametric models is not directly derived from optical measurement, the scale of the mesh and its local geometries must be used carefully in the TBP IOD.

3. EXPERIMENT

We have implemented an example of TBP DICOM file using an image-rich full-body scanning system. Two use cases of TBP DICOM are demonstrated in this section. A template and an example of the TBP DICOM file built with the open-source package "pydicom" [32] will be available in the GitHub repository[†].

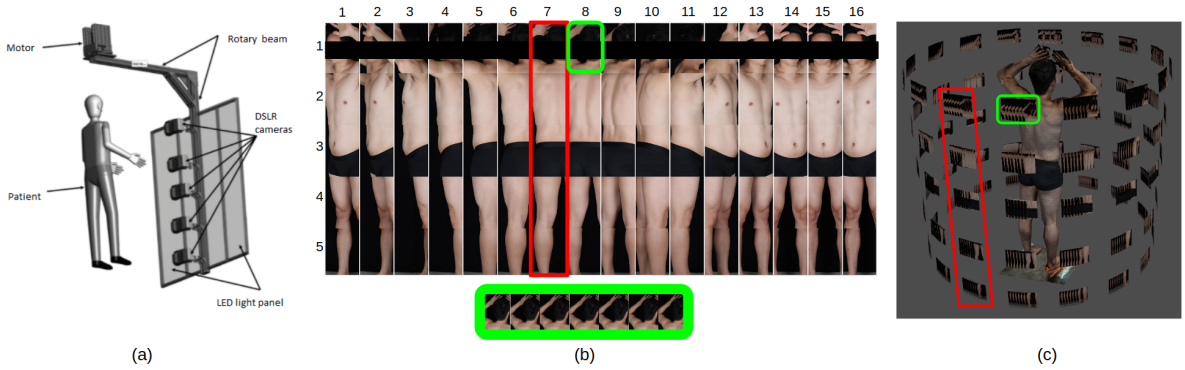

Figure 3. Overview and data of an imaging-rich TBP system

The overview of the TBP system used in the experiment is shown in Fig. 3 (a). The system consists of five DSLR cameras (Canon EOS 90D) installed on a rotary beam with motor and LED light panels for consistent

[†] https://github.com/weilunhuang-jhu/tbp_dicom

illumination. During the scan, the system rotates around the patient and captures burst of images at pre-defined angles over 360 degrees. Fig. 3 demonstrates an example of taking a burst sequence at every 22.5 degrees (16 angles in total). In Fig. 3 (b), each row displays the images from a single camera, and each column shows the images from one angle across five cameras. The green box shows an example of burst sequence for camera 1 at the 8^{th} angle. Each image has a resolution of 4640×6960.

To obtain a textured 3D surface mesh, we adopted the photogrammetry-based reconstruction with two open source software packages, OpenMVG [33] and OpenMVS [34]. To speed up the process, we resized the image by a factor of $\frac{1}{8}$. The reconstructed 3D mesh of the patient and recovered poses of image planes are shown in Fig. 3 (c). The original coordinate system from OpenMVG only requires a homogeneous transformation to be transformed to the Patient-Based Coordinate System as described in section 2.3. The estimated intrinsic parameters and distortion coefficients of cameras are temporarily stored in the TBP module as they are currently unavailable in DICOM.

Fig. 4 shows an example of anatomical record for a skin lesion. The navel is selected as the origin in the Patient-Based Coordinate System. In Fig. 4, (a) shows the 3D mesh and an annotated lesion along with its 3D-coordinate, (b) shows the same lesion with its 2D-coordinate in a regional image, and (c) includes a dermoscopic image for the upper and a close-up look of the lesion in the regional image for the lower. Since the camera poses and intrinsic parameters were estimated, once the lesion is selected in 3D space, its 2D-coordinate on any of the regional images can be mapped automatically as described in section 2.2.1.

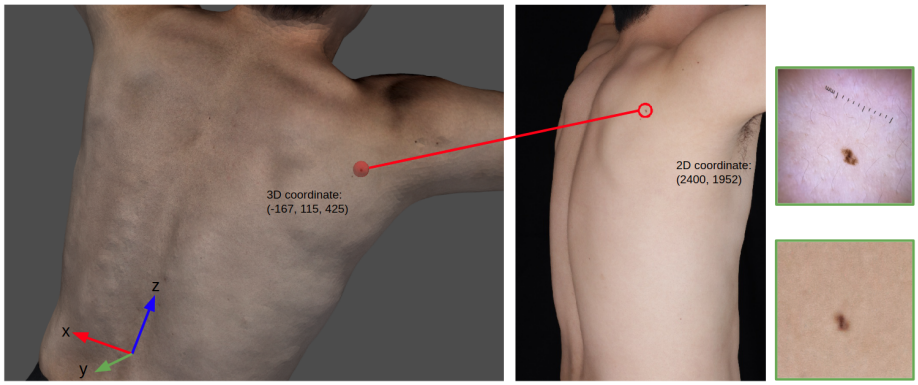

Figure 4. Anatomical record of a skin lesion in a TBP DICOM file

Fig. 5 shows an example of manual matching correspondence for four skin lesions across two scans with different poses. Four colors (blue, red, green, and yellow) are used to highlight the correspondence. The four lesions of interest are localized and annotated in two scans separately. Each lesion is assigned a **Tracking ID** (text label) and a **Tracking UID** [17]. Without sufficient anatomical context, matching the four lesions could be difficult due to the high similarity in their appearance. However, the matching task can be easily accomplished on a 3D mesh of the total body by examine their spatial structure.

4. CONCLUSION

Total Body Photography plays an important role in early melanoma detection. As various systems have been proposed, a unified format for storing data from TBP is needed for data management and beneficial for AI applications. In this paper, we provide an overview of the specific requirements and functions of TBP and an outline of the TBP IOD. We propose a structure for storing data that supports both 2D images and 3D surface mesh of the patient. A workflow is provided as a guidline to enclose TBP data. The "Work Item" is designed to not only accommodate current variants of TBP data but also be compatible with the DICOM standard for dermoscopy. Finally, the proposed structure would be applicable to future systems and other potential use of TBP. Although the proposed TBP DICOM has been experimented in an imaging-rich full-body scanning system,

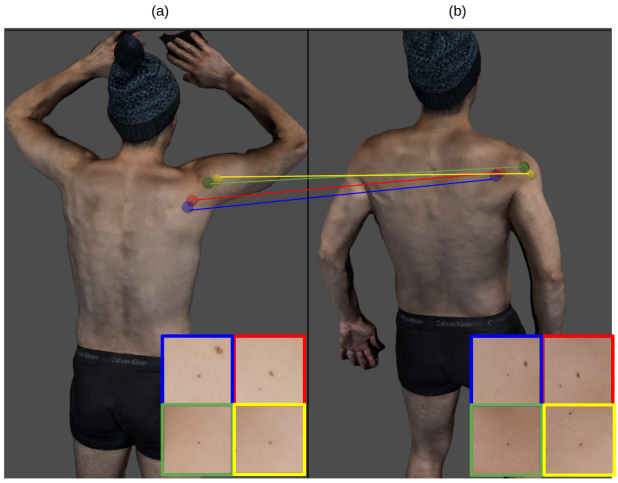

Figure 5. Skin lesions matching across scans

it needs to be implemented with more TBP systems to prove its generality in the next step. In the future, the utility of the "Work Item" description must be tested using other commercially available TBP systems in order to prepare the DICOM Supplement for TBP IOD. A more comprehensive annotation procedure for skin lesions in DICOM Structured Reports that incorporate TBP IOD and Dermoscopy IOD should be investigated for clinical applications.

ACKNOWLEDGMENTS

The research was supported by the Intramural Research Program (IRP) of the National Institute of Child Health and Human Development and the NSF 21-563 Small Business Technology Transfer (STTR) Program Phase I of National Science Foundation under Grant No. (2127051).

REFERENCES

[1] Miller, K. D., Nogueira, L., Mariotto, A. B., Rowland, J. H., Yabroff, K. R., Alfano, C. M., Jemal, A., Kramer, J. L., and Siegel, R. L., "Cancer treatment and survivorship statistics, 2019," *CA: a cancer journal for clinicians* **69**(5), 363–385 (2019).

[2] American Caner Society., "Cancer facts & figures 2021," *Atlanta: American Cancer Society* https://www.cancer.org/content/dam/cancer-org/research/cancer-facts-and-statistics/annual-cancer-facts-and-figures/2020/cancer-facts-and-figures-2020.pdf (2021). accessed: 15 December 2021.

[3] Shellenberger, R., Nabhan, M., and Kakaraparthi, S., "Melanoma screening: A plan for improving early detection," *Annals of medicine* **48**(3), 142–148 (2016).

[4] Halpern, A. C., "Total body skin imaging as an aid to melanoma detection.," in [*Seminars in cutaneous medicine and surgery*], **22**(1), 2–8 (2003).

[5] Strunck, J. L., Smart, T. C., Boucher, K. M., Secrest, A. M., and Grossman, D., "Improved melanoma outcomes and survival in patients monitored by total body photography: A natural experiment," *The Journal of dermatology* **47**(4), 342–347 (2020).

[6] Abbasi, N. R., Shaw, H. M., Rigel, D. S., Friedman, R. J., McCarthy, W. H., Osman, I., Kopf, A. W., and Polsky, D., "Early diagnosis of cutaneous melanoma: revisiting the abcd criteria," *Jama* **292**(22), 2771–2776 (2004).

[7] Gaudy-Marqueste, C., Wazaefi, Y., Bruneu, Y., Triller, R., Thomas, L., Pellacani, G., Malvehy, J., Avril, M.-F., Monestier, S., Richard, M.-A., et al., "Ugly duckling sign as a major factor of efficiency in melanoma detection," *JAMA dermatology* **153**(4), 279–284 (2017).

[8] Deinlein, T., Michor, C., Hofmann-Wellenhof, R., Schmid-Zalaudek, K., and Fink-Puches, R., "The importance of total-body photography and sequential digital dermatoscopy for monitoring patients at increased melanoma risk," *JDDG: Journal der Deutschen Dermatologischen Gesellschaft* **18**(7), 692–697 (2020).

[9] Dengel, L. T., Petroni, G. R., Judge, J., Chen, D., Acton, S. T., Schroen, A. T., and Slingluff, C. L., "Total body photography for skin cancer screening," *International Journal of Dermatology* **54**, 1250–1254 (Nov. 2015). Number: 11.

[10] Korotkov, K., Quintana, J., Puig, S., Malvehy, J., and Garcia, R., "A new total body scanning system for automatic change detection in multiple pigmented skin lesions," *IEEE transactions on medical imaging* **34**(1), 317–338 (2014).

[11] Bogo, F., Romero, J., Peserico, E., and Black, M. J., "Automated detection of new or evolving melanocytic lesions using a 3d body model," in [*International Conference on Medical Image Computing and Computer-Assisted Intervention*], 593–600, Springer (2014).

[12] Zhao, M., Kawahara, J., Shamanian, S., Abhishek, K., Chandrashekar, P., and Hamarneh, G., "Detection and longitudinal tracking of pigmented skin lesions in 3d total-body skin textured meshes," *arXiv preprint arXiv:2105.00374* (2021).

[13] Eapen, B. R., "Artificial intelligence in dermatology: A practical introduction to a paradigm shift," *Indian Dermatology Online Journal* **11**(6), 881 (2020).

[14] Caffery, L. J., Rotemberg, V., Weber, J., Soyer, H. P., Malvehy, J., and Clunie, D., "The role of dicom in artificial intelligence for skin disease," *Frontiers in medicine* **7** (2020).

[15] NEMA PS3 / ISO 12052, "Digital Imaging and Communications in Medicine (DICOM) Standard," *National Electrical Manufacturers Association, Rosslyn, VA, USA* http://www.dicomstandard.org/ . accessed: 15 December 2021.

[16] Caffery, L. J., Clunie, D., Curiel-Lewandrowski, C., Malvehy, J., Soyer, H. P., and Halpern, A. C., "Transforming dermatologic imaging for the digital era: metadata and standards," *Journal of digital imaging* **31**(4), 568–577 (2018).

[17] National Electrical Manufacturers Association., "Digital imaging and communications in medicine (dicom) supplement 221: Dermoscopy," https://www.dicomstandard.org/News/current/docs/sups/sup221.pdf (2019). accessed: 25 December 2021.

[18] Cho, T. S., Freeman, W. T., and Tsao, H., "A reliable skin mole localization scheme," in [*2007 IEEE 11th International Conference on Computer Vision*], 1–8, IEEE (2007).

[19] Soenksen, L. R., Kassis, T., Conover, S. T., Marti-Fuster, B., Birkenfeld, J. S., Tucker-Schwartz, J., Naseem, A., Stavert, R. R., Kim, C. C., Senna, M. M., et al., "Using deep learning for dermatologist-level detection of suspicious pigmented skin lesions from wide-field images," *Science Translational Medicine* **13**(581) (2021).

[20] Mirzaalian, H., Lee, T. K., and Hamarneh, G., "Skin lesion tracking using structured graphical models," *Medical image analysis* **27**, 84–92 (2016).

[21] Korotkov, K., Quintana, J., Campos, R., Jesús-Silva, A., Iglesias, P., Puig, S., Malvehy, J., and Garcia, R., "An improved skin lesion matching scheme in total body photography," *IEEE journal of biomedical and health informatics* **23**(2), 586–598 (2018).

[22] Navarro, F., Escudero-Vinolo, M., and Bescós, J., "Accurate segmentation and registration of skin lesion images to evaluate lesion change," *IEEE journal of biomedical and health informatics* **23**(2), 501–508 (2018).

[23] National Electrical Manufacturers Association., "Digital imaging and communications in medicine (dicom) supplement 154: Optical surface scanner storage sop class," https://www.dicomstandard.org/News-dir/ftsup/docs/sups/sup154.pdf (2012). accessed: 05 January 2022.

[24] Thomas, N. E., Kricker, A., From, L., Busam, K., Millikan, R. C., Ritchey, M. E., Armstrong, B. K., Lee-Taylor, J., Marrett, L. D., Anton-Culver, H., et al., "Associations of cumulative sun exposure and phenotypic characteristics with histologic solar elastosis," *Cancer Epidemiology and Prevention Biomarkers* **19**(11), 2932–2941 (2010).

[25] Veasey, J. V., Miguel, B., Bedrikow, R. B., Mota Jr, R. D. C., and Buarque, V., "Wood's lamp in dermatology: Applications in the daily practice," *Surg Cosmet Dermatol* **9**, 324–6 (2017).

[26] Borman, S. and Stevenson, R. L., "Super-resolution from image sequences-a review," in [*1998 Midwest symposium on circuits and systems (Cat. No. 98CB36268)*], 374–378, IEEE (1998).

[27] Liu, H., Ruan, Z., Zhao, P., Dong, C., Shang, F., Liu, Y., and Yang, L., "Video super resolution based on deep learning: A comprehensive survey," *arXiv preprint arXiv:2007.12928* (2020).

[28] Szeliski, R., [*Computer vision: algorithms and applications*], Springer Science & Business Media (2010).

[29] Andrew, A. M., "Multiple view geometry in computer vision," *Kybernetes* (2001).

[30] Zollhöfer, M., Stotko, P., Görlitz, A., Theobalt, C., Nießner, M., Klein, R., and Kolb, A., "State of the art on 3d reconstruction with rgb-d cameras," in [*Computer graphics forum*], **37**(2), 625–652, Wiley Online Library (2018).

[31] Cheng, Z.-Q., Chen, Y., Martin, R. R., Wu, T., and Song, Z., "Parametric modeling of 3d human body shape—a survey," *Computers & Graphics* **71**, 88–100 (2018).

[32] Mason, D., scaramallion, rhaxton, mrbean bremen, Suever, J., Vanessasaurus, Lemaitre, G., Orfanos, D. P., Panchal, A., Rothberg, A., Massich, J., Kerns, J., van Golen, K., Robitaille, T., moloney, Shun-Shin, M., pawelzajdel, Conrad, B., Mattes, M., Biggs, S., Morency, F. C., Herrmann, M. D., Meine, H., Wortmann, J., Hahn, K. S., Wada, M., Rachum, R., colonelfazackerley, ferdymercury, and huicpc0207, "pydicom/pydicom: pydicom 2.1.2," (Dec. 2020).

[33] Moulon, P., Monasse, P., Perrot, R., and Marlet, R., "OpenMVG: Open multiple view geometry," in [*International Workshop on Reproducible Research in Pattern Recognition*], 60–74, Springer (2016).

[34] Cernea, D., "OpenMVS: Multi-view stereo reconstruction library," (2020).